

Analyst

Accepted Manuscript



This is an *Accepted Manuscript*, which has been through the Royal Society of Chemistry peer review process and has been accepted for publication.

Accepted Manuscripts are published online shortly after acceptance, before technical editing, formatting and proof reading. Using this free service, authors can make their results available to the community, in citable form, before we publish the edited article. We will replace this *Accepted Manuscript* with the edited and formatted *Advance Article* as soon as it is available.

You can find more information about *Accepted Manuscripts* in the [Information for Authors](#).

Please note that technical editing may introduce minor changes to the text and/or graphics, which may alter content. The journal's standard [Terms & Conditions](#) and the [Ethical guidelines](#) still apply. In no event shall the Royal Society of Chemistry be held responsible for any errors or omissions in this *Accepted Manuscript* or any consequences arising from the use of any information it contains.



Analyst

ARTICLE

A New Class of Biocompatible Fluorescent Probe AFN for Fixed and Live Cell Imaging of Intracellular Lipid Droplets

Ashutosh Sharma,^a Shahida Umar,^a Parmita Kar,^b Kavita Singh,^c Monika Sachdev,^b and Atul Goel^{*a,d}

Received 00th January 20xx,
Accepted 00th January 20xx

DOI: 10.1039/x0xx00000x

www.rsc.org/

We discovered a new class of nontoxic, highly fluorogenic and biocompatible probe AFN for selective staining of intracellular Lipid Droplets (LDs) in both fixed and live human cervical cancer cells (HeLa) and 3T3-L1 pre-adipocytes without any background artifacts. The salient features of the probe lie in visible excitation maximum, aqueous compatibility, selectivity and its remarkable stability (for more than a week) in live cells, even better than commercially available Nile Red.

Introduction

Lipid droplets (LDs) are acknowledged as dynamic cytoplasmic organelles composed of a hydrophobic core of neutral lipids (primarily sterol esters and triacylglycerols with their relative amount varying between cell types) surrounded by a phospholipid monolayer and specific proteins.^{1,2} As opposed to being inert bodies storing excess cellular fat, cellular lipids perform a host of functions such as membrane trafficking, fusion, endocytosis, signal transduction as well as a source of energy in crisis. Almost all cells have the ability to form LDs³ and understanding lipid biology has assumed enormous importance since excessive lipid storage in LDs has been associated with the etiology of several metabolic disorders such as obesity, diabetes and atherosclerosis.^{4,5} Therefore the discovery of new selective and stable fluorescent probe as a tool to visualize, quantify and/or study the molecular dynamics of LDs is essentially required to enhance our understanding in the area of lipid cell biology.⁶

Fluorescence techniques are powerful tools for studying LDs in living cells and tissues due to their advantages such as high sensitivity and selectivity.⁷ A limited number of LDs specific fluorescent dyes have been reported,⁸⁻¹² in which Nile Red⁸ and BODIPY dyes are commonly employed.⁹ Nile Red

stains most intracellular structures,¹⁰ thus visualizing poor discernment of LDs from others cellular components and also suffers from low sensitivity because of the high background noise. BODIPY dyes, on the other hand, usually have a small Stokes shift thus induce nonradiative energy transfers causing fluorescence quenching of the excited chromophore and interference from scattered light ultimately leading to weak fluorescence and background artifacts.¹¹ To improve their selectivity and staining stability for LDs, significant efforts have been made to identify new class of dyes, however Nile Red is still the choice of many researchers.¹⁰⁻¹² Our ongoing efforts in this direction led to the identification of fluoranthene dye FLUN-550 for selective staining of intracellular LDs, however the dye exhibited excitation maximum in the ultraviolet region leading to fluorescence stability only for few hours in cells.^{12d} We envisaged that D/A fluorene and related aromatic scaffolds exhibit remarkable photophysical and optical properties^{13,14} but their aqueous incompatibility and weak/no fluorescence in water snag their biological applications.

To overcome these issues and to make them biocompatible while retaining their useful photophysical characteristics, we

Analyst Accepted Manuscript

^a Fluorescent Chemistry Lab, Medicinal and Process Chemistry Division, CSIR-Central Drug Research Institute, Lucknow 226031, India.

E-mail: atul_goel@cdri.res.in

Fax: +91-522-2771941; Tel.: +91-522-2772450

^b Division of Endocrinology, CSIR-Central Drug Research Institute, Lucknow 226031, India.

^c Electron Microscopy Unit, CSIR-Central Drug Research Institute, Lucknow 226031, India.

^d Academy of Scientific and Innovative Research, New Delhi 110001, India

†Electronic Supplementary Information (ESI) available: [Spectroscopic Characterization data, 1H, 13C NMR spectra and absorption, excitation and fluorescence data of all the compounds 8-10 in PBS and DMSO. Computed TDDFT data and Cartesian coordinate, Cytotoxicity data, materials and methods].

†Electronic Supplementary Information (ESI) available: See DOI: 10.1039/x0xx00000x

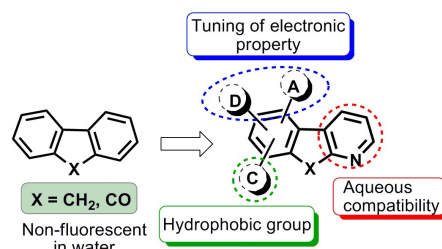
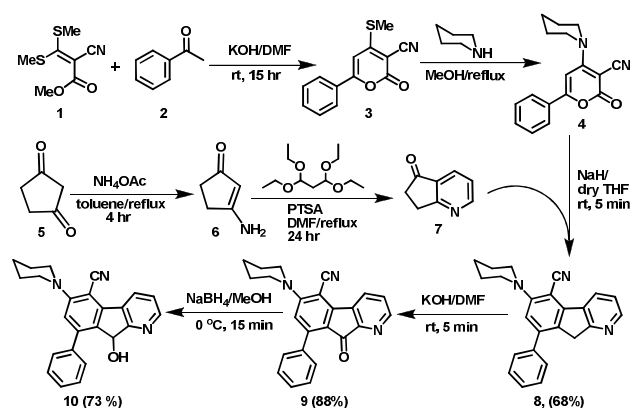


Fig. 1 Design of new donor/acceptor-based azafluorenes and azafluorenone as fluorescent bioprobe.

tailored unique donor-acceptor based azafluorene and azafluorenone by replacing one of the phenyl rings of the fluorene scaffold with its bioisostere pyridine moiety to induce an effective charge transfer with improved aqueous solubility (Fig. 1). The incorporation of donor-acceptor functionalities to modulate electronic properties of diverse skeletons has been quite successful.¹⁵⁻¹⁷ Henceforth, in this paper we report the design and synthesis of a new class of biocompatible fluorescent probe with excitation maximum in the visible region and their application in selective and stable staining of cytoplasmic lipid droplets in HeLa and 3T3-L1 pre-adipocyte cells without any background noise.

Results and Discussion

There is paucity of literature report for the synthesis of azafluorenes and azafluorenes. Few synthetic methodologies are available for these compounds, which include three-component [5 + 1] heterocyclization of 3-indanone with aryl glyoxal,^{18a} cross-coupling reaction between pyridylboronic acid and ethyl iodobenzoate followed by intramolecular cyclization,^{18b,c} photocyclisation of 2-benzoylpyridine,^{18d} one-pot DoM-Boronation-Suzuki cross coupling of azabiaryls,^{18e} and by generating a diazopyridine compound followed by photolysis in poor yield.^{18f} Recently Baran et al.^{18g} developed an efficient method to prepare mixture of azafluorenone through Pschorr-type cyclization of organotrifluoroborates in the presence of silver nitrate. In order to prepare designed donor-acceptor functionalized azafluorene (AF) and azafluorenone (AFN), we developed here a concise and highly rapid synthetic route as depicted in Scheme 1. The key intermediate 6-phenyl-2-oxo-4-methylsulfanyl-2H-pyran-3-carbonitriles (**3**) was prepared from easily accessible precursor α -oxo-ketene-*S,S*-acetal (**1**) and acetophenone (**2**) in good yield. Synthesis of azafluorenes with an amine donor and a nitrile acceptor group was achieved by preparing 6-phenyl-2-oxo-4-piperidin-1-yl-2H-pyran-3-carbonitrile (**4**) from **3** and then reacting with 6,7-dihydro-5H-cyclopenta[*b*]pyridin-5-one¹⁹ (**7**) in the presence of sodium hydride in dry THF, which furnished 8-phenyl-6-(piperidin-1-yl)-9H-indeno[2,1-*b*]pyridine-5-carbonitrile (**8**) in 68% yield. The azafluorene **8**



Scheme 1 Synthesis of 9-azafluorene, 9-azafluorenone and 9-hydroxyazafluorene

was oxidized to azafluorenone **9** in the presence of potassium hydroxide in air at room temperature. Further reduction of azafluorenone **9** with NaBH₄ furnished 9-hydroxy-azafluorene **10** in 73% yield (Scheme 1).

The photophysical properties of the synthesized compounds **8-10** in phosphate buffered saline (PBS, pH = 7.4) were examined by UV-vis absorption, excitation and fluorescence spectra (Fig. 2, Fig. S1, and Table S1, ESI†). Azafluorenes **8** and **10** showed absorption maxima at 385 nm and 352 nm respectively and fluorescence maxima at 478 nm and 465 nm respectively. To our delight, azafluorenone **9** exhibited absorption maximum at 430 nm and fluorescence maximum at 575 nm with Stokes shift of 145 nm (Fig. 2a). The quantum yields of the azafluorenes **8**, **10** and azafluorenone **9** (AFN) were found in the range of 1.4-2.6 % (in PBS) and 17-31% (in DMSO, Table S1, ESI†).

We next investigated the solvatochromic behaviour of the compounds **8-10** in a series of solvents with varying polarity index to examine the effect on the excited state. Azafluorene **8** and **10** did not show solvatochromic property while azafluorenone **9** (AFN) exhibited large solvatochromic shifts with increasing polarity from cyclohexane ($\lambda_{PL,max} = 510$ nm) to dioxane ($\lambda_{PL,max} = 535$ nm) to DCM ($\lambda_{PL,max} = 555$ nm) to ACN ($\lambda_{PL,max} = 570$ nm) to DMSO ($\lambda_{PL,max} = 592$ nm) as shown in Fig. 2b. This positive solvatochromism is mostly perceived when the dipole moment of a dye in the excited state is greater than that in the ground state during a photo-induced electronic transition, which implicates the intramolecular charge transfer (ICT) characteristic of the AFN. We observed that AFN showed high emission intensity and good fluorescence quantum yield in nonpolar solvent like cyclohexane in comparison to polar aprotic solvent like DMSO (Fig. S1, ESI†).

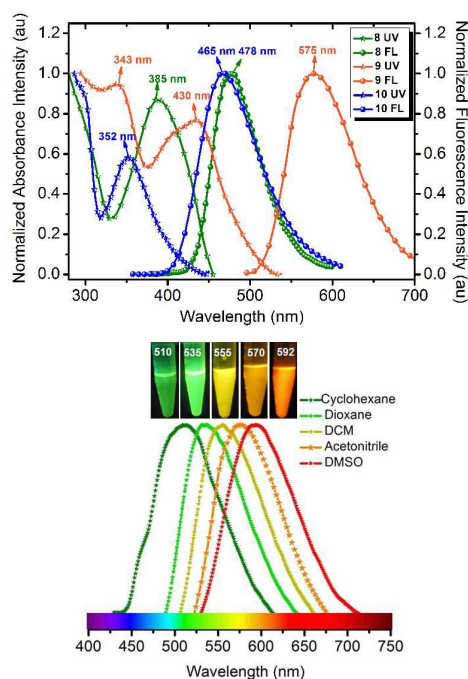


Fig. 2 (a) Absorption and emission Spectra of **8-10** in PBS (pH=7.4). (b) Emission spectrum of AFN in solvents of varying polarity.

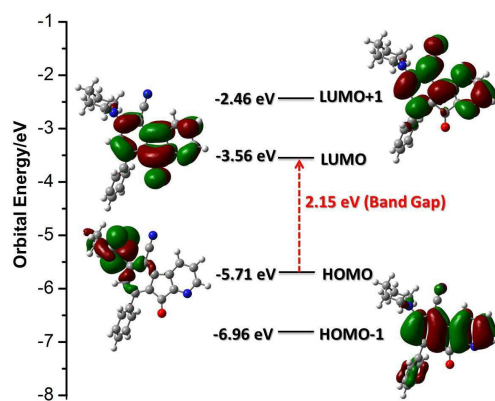


Fig. 3 Computed molecular orbital HOMO, LUMO, HOMO-1 and LUMO+1 for AFN.

To gain an insight in to the electronic properties of AFN, time-dependent density functional theory (TD-DFT) calculations were employed using a B3LYP/6-311++G(d,p) method with a Gaussian 09 package.²⁰ Molecular orbitals in the ground state for AFN are represented in Fig 3. TD-DFT calculations showed two strong transitions at 349 and 447 nm with an oscillator strength of $f = 0.1007$ and 0.0906 respectively, which correspond to HOMO-1→LUMO+1 and HOMO→LUMO respectively. The transition band at higher wavelength may be assigned to an ICT band due to charge transfer from piperidine donor moiety (HOMO) to azafluorenone acceptor moiety (LUMO). The energies of the HOMO and LUMO levels and band gap of AFN were found to be -5.71, -3.56 and 2.15 eV respectively.

Owing to the interesting photophysical properties in water, we explored the application of these compounds (**8-10**) as fluorescent probes in live and fixed cell imaging. These compounds were systematically assessed for their capability to infuse and stain the intracellular space in HeLa cells using confocal microscopy. For this purpose, fixed HeLa cells were permeabilised and incubated with different concentrations (0.1, 0.25, 0.5 and 1 μM) under growth conditions. The excess dye

was washed away with phosphate buffered saline. Confocal imaging results revealed that only azafluorenone (AFN) showed permeability and the staining in the cytosol in a specific pattern (Fig. 4A-C). Experimentation with various commercially available organelle-specific dyes revealed that the spherical objects in cytosol with distinctly bright fluorescence were lipid droplets (LDs), which showed strong co-localization with Nile red, a known commercial LDs marker (Fig. 4D-F). In order to reconfirm the LDs specific staining by AFN, we performed experiments on fixed 3T3-L1 pre-adipocytes (generally enriched in LDs) and results are shown in Fig. 4G-I. Interestingly the staining pattern implicated that the dye AFN selectively stained LDs having co-localization with Nile red (Fig. 4J-L). Overall staining pattern of AFN in fixed HeLa cells and 3T3-L1 pre-adipocytes confirmed that AFN is a fluorescent probe for selective staining of LDs without any background noise and is better than Nile Red, which showed non-specific staining in the background.²¹ We next examined the toxicity of AFN to check its biocompatibility. The cytotoxicity of the dye was assessed using 3-(4,5-dimethyl-2-thiazolyl)-2,5-diphenyltetrazolium bromide (MTT) assay. AFN showed 99% cell viability in both HeLa and 3T3-L1 up to 10 μM concentration (Fig. S2, ESI†). The excellent biocompatibility of AFN motivated us to further investigate their application in live cell imaging, which is important in the perspective of identification of various cellular processes.

Now further experiments were performed in live HeLa cells and 3T3-L1 pre-adipocyte as described in supplementary information and confocal images are shown in Fig. 5. Interestingly these results revealed that AFN is permeable in both these cell lines and is highly selective towards staining LDs present in the cytoplasmic region. The specific staining of LDs with emission in the green region (505-570 nm) was in agreement with good quantum yields observed in hexane. Further dual staining experiments with Nile Red clearly showed that compound AFN is highly selective to LDs as compared to Nile Red (Fig. 5D-F and Fig. 5J-L). To the best of our knowledge there is no literature report available so far to

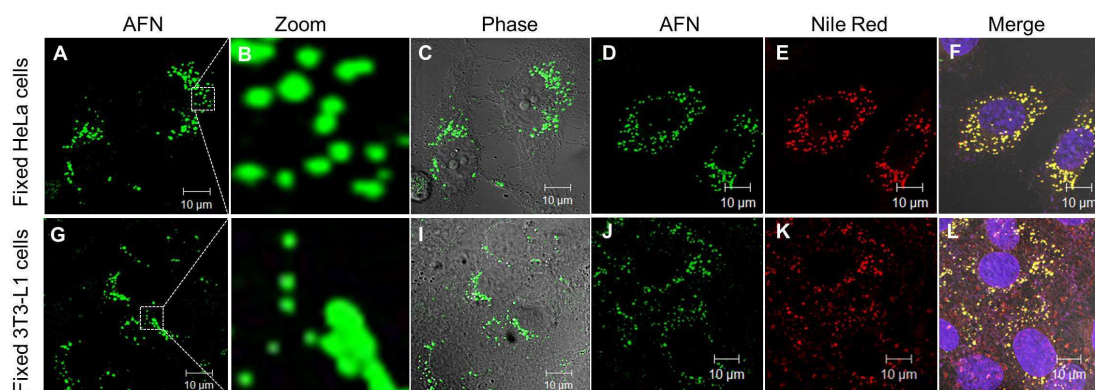


Fig. 4 Confocal fluorescence microscopy images: In fixed HeLa cells (A-C) Specific localization of LDs with AFN (0.5 μM) alone; (D-F) Co-localization of AFN (green channel, λ_{ex} 405/ λ_{em} 505-570) with Nile Red (red channel, λ_{ex} 561/ λ_{em} 575) and To-Pro (λ_{ex} 633/ λ_{em} 650). In fixed 3T3-L1 pre-adipocytes (G-I) Specific localization of LDs with AFN (0.5 μM) alone; (J-L) Co-localization of AFN with Nile Red and To-Pro.

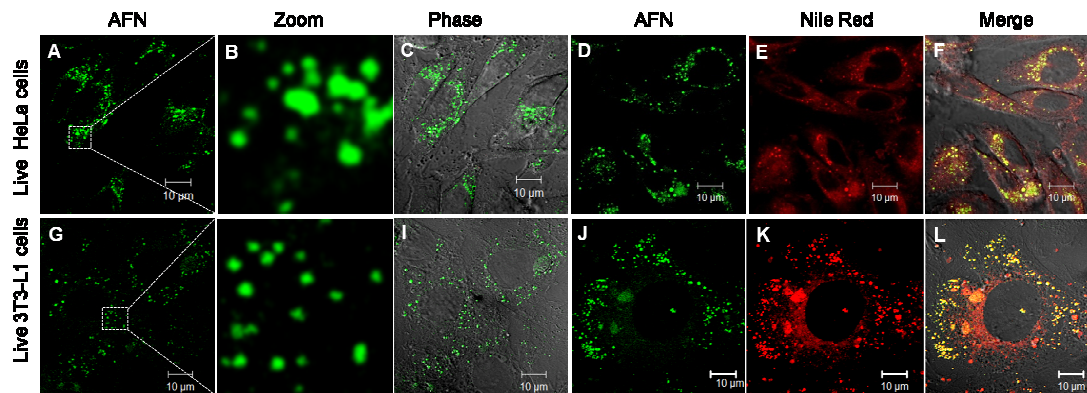


Fig. 5 (A-C) Specific localization of LDs with AFN (0.5 μM) in live HeLa cells through confocal microscopy using the laser line of 405 nm. (D-F) Co-localisation of AFN (green channel, 405 laser/505-570 BP) with Nile Red (red channel, 561 laser/575 LP) in live HeLa cells. (G-I) Specific localization of LDs with AFN (0.5 μM) in live 3T3-L1 pre-adipocyte. (J-L) Co-localisation of AFN (green channel, 405 laser/505-570 BP) with Nile Red (red channel, 561 laser/575 LP) in live 3T3-L1.

substantiate the application of azafluorenones as organelle specific fluorescent bioimaging probe.

The stability of a fluorescent probe is an important parameter in the cell imaging experiments particularly in live cell conditions, which allows researchers to get more time for analysing the test samples. Interestingly AFN showed longer staining (up to 7 days studies) as compared to Nile Red. Cells co-stained with AFN and Nile red showed quenched Nile Red staining whereas the AFN staining was still quite promising. These results implicated a unique property of the AFN dye, which proved to be more stable probe for LDs compared to the commercially available Nile Red (Fig. 6).

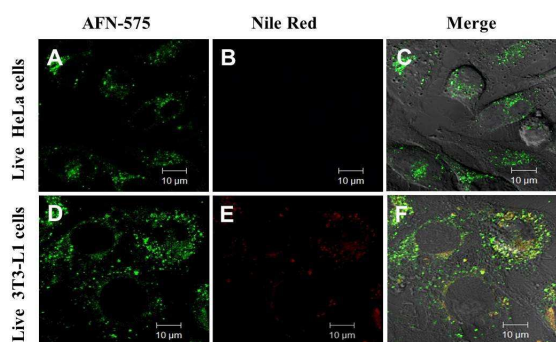


Fig. 6 Stability of AFN fluorescence in live cells, after a week through confocal microscopy after staining, the slides were stored at 4 $^{\circ}\text{C}$ for a week: Image of live HeLa cells incubated with (A) AFN (0.5 μM); (B) Nile Red (0.5 μM); (C) merge of A and B; Image of live 3T3-L1 cells incubated with (D) AFN (0.5 μM); (E) Nile Red (0.5 μM); (F) merge of D and E.

Experimental

Chemicals: DMEM media (Sigma), FBS (Gibco), DAPI (Sigma), Formaldehyde (Sigma), antibiotic Antimycotic (Gibco) solution. The stock solutions of Nile Red, AFN were prepared in analytical grade DMSO and subsequent dilutions were made using Triple Distilled Water (TDW) and PBS. The

final concentration of DMSO in the media for cell studies was used merely 0.01% v/v. Assays were performed in triplicate.

Cell Culture of HeLa and 3T3-L1: Cervical cancer cell line of HeLa and pre-adipocyte cell line of 3T3-L1 were cultured in Dulbecco's Modified Eagles Medium (DMEM) with phenol red, L-glutamine and 4.8 g/L D-glucose supplemented with 10 % heat inactivated FBS (Gibco) and Penicillin–Streptomycin (Sigma). These cells were monitored thoroughly for their density and morphology at 37 $^{\circ}\text{C}$ in CO_2 incubator. Once the cells were 70 % confluent, they were trypsinized and seeded ($\sim 10^5$) onto a coverslip and incubated overnight in CO_2 incubator. Next day morning, these cells were either fixed with 4% formaldehyde for 20 minutes or used for the treatment of AFN; at this step fixed cells can be stored at 4 $^{\circ}\text{C}$.

Staining of AFN in fixed HeLa and 3T3-L1 Cells: Fixed HeLa and 3T3L1 cells were washed with PBS and subjected to permeabilization Buffer (0.1% Tween 20, 0.05% NP-40 in PBS) for 10 min. Now these cells were washed with PBS and incubated with either 500 nM of compound AFN or 500 nM of Nile Red or both and incubated in a rocker for overnight at 4 $^{\circ}\text{C}$. After the incubation, the coverslips were washed with PBST thrice and once with PBS. The cells were then incubated with nuclear stain To-Pro (1 μM) for 25 minutes. After the nuclear staining, washing steps were performed again with PBST thrice and PBS twice. Now the coverslips having the stained adhered cells were finally mounted up-side down with Prolong gold antifade reagent (Invitrogen) on glass slides. Images were acquired on Confocal Microscope with a 63 x Plan Apochromat Oil Phase II 1.4 objective. Lasers used were Diode 405 nm for the compound AFN, DPSS 561 nm for Nile Red and Ar/ML 633 nm for the nuclear stain To-Pro. Z-stacking of images was also done.

Staining of AFN in live HeLa and 3T3-L1 Cells: Once HeLa and 3T3-L1 cells were seeded on coverslips and incubated overnight at 37 $^{\circ}\text{C}$ in CO_2 incubator. Next day morning these live cells were treated with either 500nM of compound AFN (Dissolved AFN in DMSO, the stock was made with 100 μM

concentration and the final concentration of DMSO in the media was merely 0.01% v/v) or 500 nM of Nile Red or both; and incubated further for 4 hours in CO₂ incubator. After that these coverslips were washed with 10% FBS (Gibco) in PBST thrice and twice with PBS. After the staining, these cells were fixed now with 4% formaldehyde and mounted up-side down with Prolong gold antifade reagent (Invitrogen) on glass slides. The Images were acquired on Confocal Microscope with a 63 x Plan Apochromat Oil Phase II 1.4 objective. Lasers used were Diode 405 nm for the compound AFN and DPSS 561 nm for Nile Red.

Cell Viability Assay after the treatment of AFN through MTT: Yellow MTT [3-(4, 5-Dimethylthiazol-2-yl)-2,5-diphenyl-tetrazolium bromide (Sigma), a tetrazolium compound is reduced to purple formazan in the mitochondria of living cells. The absorbance of this colored solution can be quantified at certain wavelength (usually between 500 and 600 nm) through a spectrophotometer. When the amount of purple formazan produced by cells treated with an agent is compared with the amount of formazan produced by untreated control cells, if the effectiveness of the agent is causing death of cells can be deduced, through the production of a dose-response curve. To check whether there is any cytotoxicity of the compound AFN, MTT assay was performed in 96 well viable cells in triplicate were treated with AFN in a range of 50nM to 10 μ M. The cells were trypsinized and counted in a hemocytometer to seed about 10,000 per well and incubated overnight in CO₂ incubator. Next day morning, these cells were treated with the compound AFN and incubated further for 24 hrs in CO₂ incubator. Now 20 μ l of 5 mg/ml MTT was added to each well and the plate was incubated for 4 hours at 37°C in culture hood. After that the media was carefully removed and the reaction was stopped using 200 μ l MTT solvent. The plate was covered and agitated on orbital shaker for 15 minutes; now absorbance was read at 570 nm. The Optical Density (O.D.) of the MTT containing wells was used to generate percent viability of the cells in presence of various concentration of A261 dye to access the toxic effect of AFN. To calculate the percent viability of the cells, the O.D. for 0 nM of AFN was considered as 100% viability and the corresponding values for other AFN concentrations were calculated.

Instrumentation: ¹H and ¹³C NMR spectra were taken at 300 MHz and 400 MHz respectively. CDCl₃ and DMSO-*d*₆ were taken as solvents. Chemical shifts are reported in parts per million shift (δ -value) from Me₄Si (δ 0 ppm for ¹H) or based on the middle peak of the solvent (CDCl₃) (δ 77.00 ppm for ¹³C NMR) as an internal standard. Signal pattern are indicate as s, singlet; brs, broad singlet; d, doublet; t, triplet; m, multiplet. Coupling constant (*J*) are given in hertz. Infrared (IR) spectra were recorded in KBr disc and reported in wave number (cm⁻¹). The ESI-MS were recorded on MICROMASS Quadro-II LCMS system. The HRMS spectra were recorded as ESI-HRMS on a mass analyzer system. All the reactions were monitored by TLC and visualization was done with UV light (254 nm).

General procedure for the synthesis of 3 and 4: A mixture of methyl 2-cyano-3,3-dimethylsulfanylacrylate **1** (10 mmol), acetophenone **2** (11 mmol) and powdered KOH (12 mmol) in DMSO (50 mL) was stirred at room temperature for 14 h. After completion, the reaction mixture was poured into ice water with constant stirring. The precipitate thus obtained was filtered and purified on a silica gel column using chloroform as eluent to yield 6-aryl-2-oxo-4-methylsulfanyl-2*H*-pyran-3-carbonitriles **3**. The compound **3** (1 mmol) was refluxed in methanol with a secondary amine (piperidine, 1.2 mmol) for 6 h, the reaction mixture was cooled to room temperature and the solid obtained was filtered to furnish 6-aryl-2-oxo-4-piperidin-1-yl-2*H*-pyran-3-carbonitriles **4** in good yield.²²

Synthesis of 8-phenyl-6-(piperidin-1-yl)-9*H*-indeno[2,1-*b*]pyridine-5-carbonitrile (8**):** A mixture of 2-oxo-6-phenyl-4-(piperidin-1-yl)-2*H*-pyran-3-carbonitrile (280 mg, 1 mmol), 6,7-dihydro-5*H*-cyclopenta[*b*]pyridin-5-one (133 mg, 1 mmol) and NaH (60% dispersion in oil, 60 mg, 1.5 mmol) in dry THF (5 ml) was stirred at room temperature for 5 min. The progress of reaction was monitored by TLC and on completion, solvent was evaporated and reaction mixture was poured onto crushed ice with vigorous stirring and finally neutralized with 10% HCl. The precipitate obtained was filtered and purified on a silica gel column using 5% ethyl acetate in *n*-hexane as the eluent to afford 237 mg (68%) as a light yellow solid: *R*_f = 0.56 (ethyl acetate/*n*-hexane, 1:9, v/v); mp (ethyl acetate/*n*-hexane) 166-168 °C; MS (ESI) 352 [M + H]⁺; IR (KBr) ν = 2216 (CN) cm⁻¹; ¹H NMR (300 MHz, CDCl₃): δ = 8.76-8.83 (m, 1H), 8.54-8.59 (m, 1H), 7.45-7.54 (m, 5H), 7.34-7.44 (m, 1H), 7.01 (s, 1H), 3.98 (s, 2H), 3.24 (t, *J* = 5.0 Hz, 4H), 1.83-1.95 (m, 4H), 1.62-1.69 (m, 2H); ¹³C NMR (50 MHz, CDCl₃): δ = 165.3, 157.6, 148.9, 143.9, 142.6, 139.7, 133.0, 132.7, 129.8, 128.8, 128.4, 128.3, 122.0, 118.5, 117.6, 98.5, 53.8, 37.8, 26.2, 24.1 ppm; HRMS calculated for C₂₄H₂₂N₃ [M⁺ + H] 352.1814, found: 352.1805.

Synthesis of 9-oxo-8-phenyl-6-(piperidin-1-yl)-9*H*-indeno[2,1-*b*]pyridine-5-carbonitrile (9**; AFN):** A solution of 8-phenyl-6-(piperidin-1-yl)-9*H*-indeno[2,1-*b*]pyridine-5-carbonitrile (351 mg) in DMF (5 mL) was added potassium hydroxide (84 mg, 1.5 mmol) and the solution was stirred at 25 °C in air for less than five min. After completion, the reaction solvent was evaporated under vacuum and the crude solid obtained was quenched with ice water and subsequently neutralized by dilute HCl. The precipitate obtained was filtered and purified on a silica gel column using 10% ethyl acetate in *n*-hexane as the eluent to afford 320 mg (88%) as a light brown solid: *R*_f = 0.52 (ethyl acetate/*n*-hexane, 1:9, v/v); mp (ethyl acetate/*n*-hexane) 172-174 °C; MS (ESI) 366 [M + H]⁺; IR (KBr) ν = 2208 (CN), 1718 (C=O) cm⁻¹; ¹H NMR (300 MHz, CDCl₃): δ = 8.62-8.70 (m, 2H), 7.43-7.55 (m, 5H), 7.37-7.46 (m, 1H), 6.71 (s, 1H), 3.46 (t, *J* = 5.2 Hz, 4H), 1.79-1.85 (m, 4H), 1.68-1.75 (m, 2H); ¹³C NMR (100 MHz, CDCl₃): δ = 187.5, 159.8, 153.5, 151.4, 148.5, 147.3, 136.4, 135.9, 129.5, 129.2, 128.9, 128.0, 126.6, 120.2, 119.8, 116.9, 96.0, 52.5, 25.8, 23.8 ppm; HRMS calculated for C₂₄H₂₀N₃O [M⁺ + H] 366.1606, found: 366.1579.

Synthesis of 9-hydroxy-8-phenyl-6-(piperidin-1-yl)-9H-indeno[2,1-b]pyridine-5-carbonitrile (10): A solution of 8-phenyl-6-(piperidin-1-yl)-9H-indeno[2,1-b]pyridine-5-carbonitrile (367 mg, 1 mmol) in methanol (5 mL) was added sodium borohydride (75 mg, 2 mmol) and the solution was stirred at 0° C for 30 min. After completion, the reaction solvent was evaporated under vacuum and the crude solid obtained was quenched with ice water and subsequently neutralized by dilute HCl. The precipitate obtained was filtered and purified on a neutral alumina column using 20% ethyl acetate in *n*-hexane as the eluent to afford 268 mg (73%) as a brown solid: $R_f = 0.42$ (ethyl acetate /*n*-hexane, 1:9, v/v); mp (ethyl acetate /*n*-hexane) 186-188 °C; MS (ESI) 368 [M + H]⁺; IR (KBr) $\nu = 2209$ (CN), 3437 (OH) cm⁻¹; ¹H NMR (300 MHz, CDCl₃): $\delta = 8.67$ (d, $J = 7.7$ Hz, 1H), 8.36-8.42 (m, 1H), 7.60-7.66 (m, 2H), 7.46-7.56 (m, 3H), 7.32-7.39 (m, 1H), 6.92 (s, 1H), 5.75 (s, 1H), 3.92 (brs, 1H), 3.20-3.30 (m, 4H), 1.78-1.88 (m, 4H), 1.59-1.69 (m, 2H) ppm; ¹³C NMR (100 MHz, CDCl₃): $\delta = 153.6, 151.5, 148.9, 147.5, 145.0, 136.5, 129.6, 129.2, 128.9, 128.7, 128.4, 128.1, 126.7, 123.9, 120.3, 119.8, 98.4, 52.6, 25.9, 23.9$ ppm; HRMS calculated for C₂₄H₂₂N₃O [M⁺ + H] 368.1763, found: 368.1755.

Conclusion

In conclusion we have designed and developed an efficient methodology for the synthesis of donor-acceptor appended azafluorenes and azafluorenone using easily accessible precursors. We also discovered a new class of fluorescent probe azafluorenone AFN, which is a nontoxic, highly selective and stable dye for staining LDs in different cell lines (fixed/live HeLa cells and 3T3-L1 pre-adipocyte). This new LD-specific biocompatible fluorescent probe AFN with visible excitation and distinct emission band has opened new avenues for analysing LDs in cancer containing tissue samples and real time monitoring of LDs functions in lipid cell biology. Current work in this direction is in progress.

Acknowledgements

The work is supported by the CSIR, New Delhi under Network project BSC0102 and BSC0114. The manuscript reference number for the CSIR-CDRI is 337/2015/AG.

Notes and References

- (a) M. R. Wenk, P. D. Camilli, *Proc. Natl. Acad. Sci. U. S. A.*, 2004, **101**, 8262-8269; (b) J. C. Fernandez-Checa, *Biochem. Biophys. Res. Commun.*, 2003, **304**, 471-479.
- T. C. Walther, R. V. Farese, *Annu. Rev. Biochem.*, 2012, **81**, 687-714.
- C. W. Roberts, R. M. Leod, D. W. Rice, M. Ginger, M. L. Chance, L. J. Goad, *Mol. Biochem. Parasitol.*, 2003, **126**, 129-142.
- S. Calandra, P. Tarugi, H. E. Speedy, A. F. Dean, S. Bertolini, C. C. Shoulders, *J. Lipid Res.*, 2011, **52**, 1885-1962.
- B. M. Spiegelman, J. S. Flier, *Cell*, 2001, **104**, 531-543.
- (a) A. B. Neef, C. Schultz, *Angew. Chem. Int. Ed.*, 2009, **48**, 1498-1500; (b) N. P. Damayanti, L. L. Parker, J. M. K. Irudayaraj, *Angew. Chem. Int. Ed.*, 2013, **52**, 3931-3943.
- S. M. Borisov and O. S. Wolfbeis, *Chem. Rev.*, 2008, **108**, 423.

- (a) P. Greenspan, E. P. Mayer and S. D. Fowler, *J. Cell Biol.*, 1985, **100**, 965-973; (b) K. S. Jones, A. P. Alimov, H. L. Rilo, R. J. Jandacek, L. A. Woollett and W. T. Penberthy, *Nutr. Metab.*, 2008, **5**, 23.
- J. Spandl, D. J. White, J. Peychl and C. Thiele, *Traffic*, 2009, **10**, 1579-1584; (b) Y. Ohsaki, Y. Shinohara M. Suzuki and T. Fujimoto, *Histochem. Cell Biol.*, 2010, **133**, 477480.
- P. M. Goczke and D. A. Freeman, *Cytometry*, 1994, **17**, 151-158.
- A. Loudet and K. Burgess, *Chem. Rev.*, 2007, **107**, 4891-4932.
- (a) J. H. Lee, J.-H. So, J. H. Jeon, E. B. Choi, Y.-R. Lee, Y.-T. Chang, C.-H. Kim, M. A. Bae, J. H. Ahn, *Chem. Commun.* 2011, **47**, 7500-7502; (b) H. J. Yang, C. L. Hsu, J. Y. Yang, W. Y. Yang, *PLoS One* 2012, **7**, e32693; (c) E. Kim, S. Lee, S. B. Park, *Chem. Commun.* 2012, **48**, 2331-2333. (d) A. Goel, A. Sharma, M. Kathuria, A. Bhattacharjee, A. Verma, P. R. Mishra, A. Nazir, K. Mitra, *Org. Lett.* 2014, **16**, 756-759.
- (a) C. Qin, A. Islam and L. Han, *J. Mater. Chem.*, 2012, **22**, 19236-19243; (b) X.-H. Zhou, Y. Zhang, Y.-Q. Xie, Y. Cao and Jian Pei, *Macromolecules*, 2006, **39**, 3830-3840.
- (a) A. Goel, S. Chaurasia, M. Dixit, V. Kumar, S. Prakash, B. Jena, J. K. Verma, M. Jain, R. S. Anand, S. S. Manoharan, *Org. Lett.*, 2009, **11**, 1289-1292; (b) A. Goel, S. Chaurasia, V. Kumar, R. S. Anand, S. Manoharan, S. PCT WO/2009/122445 dated 08.10.2009.
- (a) Z. M. Hudson, S. Wang, *Acc. Chem. Res.*, 2009, **42**, 1584-1596. (b) H. J. Kim, C. H. Heo, H. M. Kim, *J. Am. Chem. Soc.*, 2013, **135**, 17969-17977; (c) X. H. Jin, C. Chen, C. X. Ren, L. X. Cai, J. Zhang, *Chem. Commun.*, 2014, **50**, 15878-15881; (d) Y. I. Park, C.Y. Kuo, J. S. Martinez, Y. S. Park, O. Postupna, A. Zhugayevych, S. Kim, J. Park, S. Tretiak, H. L. Wang, *ACS Appl. Mater. Interfaces*, 2013, **5**, 4685-4695.
- (a) Q. Li, M. Peng, H. Li, C. Zhong, L. Zhang, X. Cheng, X. Peng, Q. Wang, Q. Jingui, Z. Li, *Org. Lett.*, 2012, **14**, 2094-2097; (b) J. Dhuguru, W. Liu, W. G. Gonzalez, W. M. Babinchak, J. Miksovskaa, R. Landgraf, J. N. Wilson, *J. Org. Chem.* 2014, **79**, 4940-4947; (c) G. Feng, J. Liu, R. Zhang, B. Liu, *Chem. Commun.*, 2014, **50**, 9497-9500.
- (a) A. Goel, S. Umar, P. Nag, A. Sharma, L. Kumar, Shamsuzzama, Z. Hossain, J. R. Gayen, A. Nazir, *Chem. Commun.*, 2015, **51**, 5001-5004; (b) A. Goel, A. Sharma, M. Rawat, R. S. Anand, R. Kant, *J. Org. Chem.*, 2014, **79**, 10873-10880; (c) A. Goel, V. Kumar, S. P. Singh, A. Sharma, S. Prakash, C. Singh, R. S. Anand, *J. Mater. Chem.*, 2012, **22**, 14880-14888; (d) A. Goel, V. Kumar, P. Nag, V. Bajpai, B. Kumar, C. Singh, S. Prakash, R. S. Anand, *J. Org. Chem.*, 2011, **76**, 7474-7481; (e) A. Goel, V. Kumar, S. Chaurasia, M. Rawat, R. Prasad, R. S. Anand, *J. Org. Chem.*, 2010, **75**, 3656-3662.
- (a) Y. Li, W. Fan, H.-W. Xu, B. Jiang, S.-L. Wang, S.-J. Tu, *Org. Biomol. Chem.*, 2013, **11**, 2417-2420; (b) A.-S. Rebstock, F. Mongin, F. Tricourt, G. Queguiner, *Tetrahedron*, 2003, **59**, 4973-4997; (c) D. Tilly, A.-S. Castanet, J. Mortier, *Tetrahedron Lett.*, 2006, **47**, 1121-1123; (d) Y. Du, J. Xue, M.-De Li, X. Guan, D.W. McCamant, D. L. Phillips, *Chem. Eur. J.*, 2010, **16**, 6961-6972. (e) M. Alessi, A. L. Larkin, K. A. Ogilvie, L. A. Green, S. Lai, S. Lopez and V. Snieckus, *J. Org. Chem.*, 2007, **72**, 1588-1594; (f) E. P. Kyba, S.-T. Liu, K. Chockalingam, and B. R. Reddy, *J. Org. Chem.* 1988, **53**, 3513-3521; (g) J. W. Lockner, D. D. Dixon, R. Risgaard, P. S. Baran, *Org. Lett.*, 2011, **13**, 5628-5631.
- Y. Huang, R. W. Hartmann, *Synthetic Commun.*, 1998, **28**, 1197-1200.
- M. J. Frisch, G. W. Trucks, H. B. Schlegel, G. E. Scuseria, M. A. Robb, J. R. Cheeseman, G. Scalmani, V. Barone, B. Mennucci, G. A. Petersson, H. Nakatsuji, M. Caricato, X. Li, H. P. Hratchian, A. F. Izmaylov, J. Bloino, G. Zheng, J. L. Sonnenberg, M. Hada, M. Ehara, K. Toyota, R. Fukuda, J. Hasegawa, M. Ishida, T. Nakajima, Y. Honda, O. Kitao, H. Nakai, T. Vreven, J. A. Montgomery, Jr, J. E. Peralta, F. Ogliaro, M. Bearpark, J. J. Heyd, E. Brothers, K. N. Kudin, V. N. Staroverov, T. Keith, R. Kobayashi, J. Normand, K. Raghavachari, A. Rendell, C. Burant, S. S. Iyengar, J. Tomasi, M.

Journal Name

ARTICLE

- 1
2
3 Cossi, N. Rega, J. M. Millam, M. Klene, J. E. Knox, J. B. Cross, V.
4 Bakken, C. Adamo, J. Jaramillo, R. Gomperts, R. E. Stratmann, O.
5 Yazyev, A. J. Austin, R. Cammi, C. Pomelli, J. W. Ochterski, R. L.
6 Martin, K. Morokuma, V. G. Zakrzewski, G. A. Voth, P. Salvador,
7 J. J. Dannenberg, S. Dapprich, A. D. Daniels, O. Farkas, J. B.
8 Foresman, J. V. Ortiz, J. Cioslowski and D. J. Fox, Gaussian 09
9 (*Revision D.01*), Gaussian, Inc., Wallingford CT, 2013.
10 21. E. J. O'Rourke, A. A. Soukas, C. E. Carr and G. Ruvkun, *Cell*
11 *Metab.*, 2009, **10**, 430-435.
12 22. N. Mizuyama, Y. Murakami, S. Kohra, K. Ueda, K. Hiraoka, J.
13 Nagaoka, K. Takahashi, Y. Shigemitsu; Y. Tominaga *J.*
14 *Heterocyclic Chem.*, 2007, **44**, 115-132.
15
16
17
18
19
20
21
22
23
24
25
26
27
28
29
30
31
32
33
34
35
36
37
38
39
40
41
42
43
44
45
46
47
48
49
50
51
52
53
54
55
56
57
58
59
60